

# Mitigation of SSCI-Driven Complex Oscillations using Dynamic Virtual Impedance Based Control

Taimur Zaman<sup>1</sup>, Zhiwang Feng<sup>1</sup>, Mazheruddin Syed<sup>2</sup>, and Graeme Burt<sup>1</sup>

<sup>1</sup>Department of Electronic and Electrical Engineering, University of Strathclyde, Glasgow, United Kingdom

<sup>2</sup>Energy Advisory, WSP, Glasgow, United Kingdom

{taimur.zaman, zhiwang.feng, graeme.burt}@strath.ac.uk, mazher.syed@wsp.com

**Abstract**—It is widely recognized that subsynchronous resonance (SSR) and control interactions (SSCI) in a power network with doubly fed induction generators (DFIGs) lead to distinct types of oscillations and that mitigating these oscillations in finite time is essential for reliable operations. Among the control approaches proposed for mitigating these oscillations, the incorporation of damping control (DC) in the  $dq$  control scheme of DFIGs is considered cost-effective and reliable. However, DC exhibits inadequate performance when the oscillations emerge with complex and non-stationary components, presenting an unascertainable bandwidth of modes. To facilitate the DC-assisted DFIG control with adaptivity to variant modes of oscillations, this paper proposes the incorporation of a single-layer feed-forward learning-based damping control strategy. The approach dynamically responds to any SSR or SSCI event and reshapes the impedance to prevent the initiation of oscillations in finite time. The viability of the proposed approach is proved by simulations and various test cases, and these demonstrate the feasibility and applicability of the proposed approach to real-world application for the first time.

**Index Terms**—Adaptive DFIG control, neural networks, power network, oscillation mitigation, subsynchronous resonance

## I. INTRODUCTION

The widespread adoption of renewable energy sources (RES) has significantly contributed to reducing the reliance on conventional power sources. However, the fast-paced transition to inverter-based resources (IBRs) has posed significant challenges to power system stability, with power system oscillations (PSO) emerging particularly as a notable concern [1]. Oscillations in power systems are frequently reported and categorized as either forced or natural oscillations. The forced oscillations are primarily related to the sub-cyclic power sources while natural oscillations can be further classified into low-frequency and SSR based oscillations. The low-frequency oscillations (LFOs) are associated to the synchronous generators (SGs) and have frequencies well below 1 Hz, whereas the SSR oscillations present a varying range of frequencies [2]. Reported literature suggests that SSR oscillations in a power network arise from the resonance interaction between the SGs and network compensators installed in weak grids. These oscillations are reported as stationary in nature and have only a single mode of frequency. However, apart from the LFOs with stationary modes, distinct oscillations with coupled frequencies and complex modes are reported as a consequence of subsynchronous control interaction (SSCI)

in the power network. It is widely recognized that these oscillations originate mainly due to changes in the network topology as a result of line reclosers or faults, and inadequate response of IBR's control to disturbances and uncertainties [1], [3].

The frequent reporting of these oscillations has led to a growing interest in the development of solutions for their mitigation. The mitigation schemes can be divided into three categories based on the structure of the control, its response and requirements for implementation [4]. The first category involves deriving a detailed model of the system and replacing the conventional PI control with states-dependent nonlinear controllers as reported in [5]–[8]. These approaches are explicitly reliant on detailed modelling of the system and involve linearization of the states. The major drawback of these methods is their complex implementation and requirement of computationally intensive control resources. It is also important to note that, the linearized models omit the high dimensionality and nonlinearity of the complex IBR system making it more sensitive to perturbations [5]. The second category of approaches involves the parameters of the conventional control being made adaptive to enhance the damping performance of the control loop. However, the dependence on a single control loop and the explicit variation of its parameters for enhancing damping performance can degrade the low voltage ride-through (LVRT) capability and dynamic performance of the system for varying operating conditions. The third and most effective approach to date involves the addition of an ancillary damping control loop activated with the detection of SSR frequencies, and damping oscillations by mitigating the effect of SSR on the phase of the signal [4], [9], [10]. This conventional subsynchronous damping control (CSDC) involves the integration of filters of specific bandwidth to filter the SSR modes and provide adjustments to the phase through lag/lead compensations. Therefore, the viability of such methods is rigorously dependent on the prior knowledge of SSR frequencies.

The practical implementation of frequency-dependent CSDC shows limited viability for non-stationary and complex frequencies, as determining the exact frequency modes and phase requires intelligent algorithms [3]. To avoid the dependency on frequency bandwidths, this work proposes a dynamic virtual impedance controller (DVIC), where a single-

layer feed-forward learning-based algorithm is employed to mitigate SSCI-driven oscillations in finite time [11]. The key contributions of the proposed method are threefold: (i) firstly, the proposed method is as simple as CSDC in structure and independent on the model states, making the implementation of the approach straightforward, (ii) prior knowledge of SSR modes and frequency bandwidths is not required as the DVIC is only based on the  $dq$  currents, and (iii) the proposed approach is adaptive and adjusts the rotor side converter (RSC) impedance in finite time by injecting a compensated signal to the  $dq$  control loop, making it stable for all varying conditions.

The rest of the paper is organized as follows; Section II describes the mathematical model of the DFIG for series compensated weak grids and the limitations of CSDC. Section III discusses the prerequisites of the proposed method and its working mechanism. The viability and effectiveness of the proposed method are evaluated in section IV. Finally, section V provides the conclusions.

## II. DFIG MODELING AND DAMPING CONTROLLER

### A. DFIG and Converter Modeling

The DFIG system is strongly coupled and requires detailed modelling when designing a control that efficiently mitigates the complex SSCI oscillations. It is best to consider the internal dynamics of DFIG with the rotor and its control extorting the system stability with changing dynamics of the grid. Fig.1 shows the DFIG connected to the grid through the grid following converter (GFLC) topology. The GFLC is employed at both sides of the DFIG as a RSC and grid side converter (GSC) with an induction generator (IG) connected through a shaft system. The IG can be represented in  $dq$  frame as [5],

$$\begin{aligned} v_{ds} &= \hat{R}_s I_{ds} + \frac{d}{dt} \psi_{ds} - \omega_s \psi_{qs} \\ v_{qs} &= \hat{R}_s I_{qs} + \frac{d}{dt} \psi_{qs} + \omega_s \psi_{ds} \\ v_{dr} &= \hat{R}_r I_{dr} + \frac{d}{dt} \psi_{dr} + \omega_{slip} \psi_{qr} \\ v_{qr} &= \hat{R}_r I_{qr} + \frac{d}{dt} \psi_{qr} + \omega_{slip} \psi_{dr} \end{aligned} \quad (1)$$

with

$$\begin{aligned} \psi_{ds} &= \hat{L}_s I_{ds} + M I_{dr}, \quad \psi_{qs} = \hat{L}_s I_{qs} + M I_{qr} \\ \psi_{dr} &= \hat{L}_r I_{dr} + M I_{ds}, \quad \psi_{qr} = \hat{L}_r I_{qr} + M I_{qs} \end{aligned}$$

where the subscript  $r, s$  refers to the rotor and stator side variables in the  $dq$  reference frame, respectively; with  $\psi, M, I, v$  and  $\omega_s$  as the flux linkage, magnetizing inductance, current, voltage and angular frequency, respectively. The equivalent resistance at stator side  $\hat{R}_s$  and inductance  $\hat{L}$  at both sides with dynamics of a compensated transmission line can be expressed as

$$\begin{aligned} \hat{R}_s &= R_s + R_{TL}, \quad \hat{L}_r = L_r - M^2 / \hat{L}_s \\ \hat{L}_s &= L_s + L_{TL} + L_{TL} - 1 / (\omega_s^2 C_s) \end{aligned} \quad (2)$$

where  $R_{TL}, L_{TL}$  and  $C_s$  refer to the resistance and, inductance of the transmission line and capacitance of the series

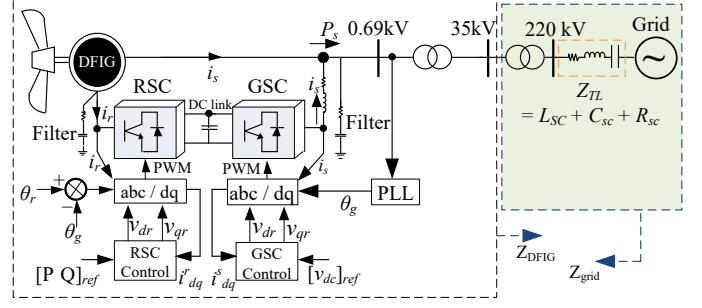


Fig. 1: A representation of weak grid with DFIG and line compensator, respectively. The RSC dynamics can be obtained from (1) and (2) as,

$$\begin{aligned} v_{dr} &= R_r I_{rd} + \hat{L}_r \frac{d}{dt} I_{rd} - \omega_{slip} \hat{L}_r I_{rq} \\ &+ \frac{M}{\hat{L}_s} \left[ v_s - \hat{R}_s I_{sd} + \omega_s \left( \hat{L}_s I_{sq} + M I_{rq} \right) \right] \\ v_{qr} &= \hat{R}_r I_{rq} + \hat{L}_r \frac{d}{dt} I_{qr} + \omega_{slip} \hat{L}_r I_{rd}, \\ &+ \frac{M}{\hat{L}_s} \left[ -\hat{R}_s I_{sq} - \omega_s \left( \hat{L}_s I_{sd} + M I_{rd} \right) \right] \end{aligned} \quad (3)$$

From (1) and (3), the equation for the electromagnetic torque,  $T_{em}$  can be derived by using the shaft dynamics and generator's current [12] as

$$T_{em} = \frac{3 N_p M v_s}{2 \omega_s \hat{L}_s} (\psi_{qs} I_{dr} - \psi_{ds} I_{qr}) \quad (4)$$

This can be further simplified by considering the alignment of  $q$ -axis flux linkage to the  $d$ -axis of the generator in the  $dq$  frame. Taking  $\psi_{ds} = \psi_s$ , the electromagnetic torque can be obtained as

$$T_{em} = \frac{N_p M v_s}{\omega_s \hat{L}_s} I_{qr} \quad (5)$$

Assuming a constant stator flux with negligible stator resistance, the current dynamics of RSC side can be obtained by considering  $v_s = \omega_s \psi_s$  and  $V_{ds} = 0$  and applying Kirchhoff's current law (KCL) as

$$\begin{aligned} \dot{I}_{dr} &= \frac{1}{\sigma \hat{L}_r} (v_{dr} - \hat{R}_r I_{dr} + S \hat{L}_r \omega_s I_{qr} \sigma) \\ \dot{I}_{qr} &= \frac{1}{\sigma \hat{L}_r} (V_{qr} - \hat{R}_r I_{qr} - S \hat{L}_r \omega_s I_{dr} \sigma) \end{aligned} \quad (6)$$

where  $\sigma = 1 - \frac{M}{L_r L_s}$ , and  $S$  is the DFIG slip given by  $S = \frac{\omega_s - \omega_r}{\omega_s}$ . Similarly, the dynamics for GSC side current are

$$\begin{aligned} \dot{I}_{ds} &= \omega_s I_{qs} + \frac{1}{L_f} (V_{dc} u_d - R_f I_{ds} - v_{ds}) \\ \dot{I}_{qs} &= \omega_s I_{ds} + \frac{1}{L_f} (V_{dc} u_q - R_f I_{qs} - v_{qs}) \end{aligned} \quad (7)$$

where,  $L_f, R_f$  represent the inductance and resistance of grid-side filters. The control inputs for GSC are denoted by  $u_d$  and  $u_q$ ; and  $v_s, I_s$  denotes the GSC voltage and current, respectively. The voltage across the series compensator can be written as

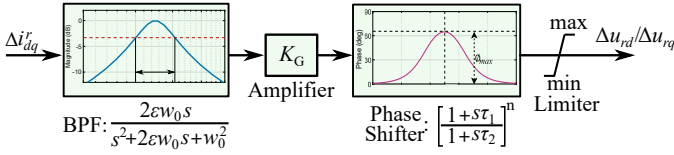


Fig. 2: Block diagram of CSDC based approach for SSR mitigation.

$$\begin{aligned} \dot{V}_{scd} &= \omega_s V_{scq} + \frac{i_d T}{C_{sc}} \\ \dot{V}_{scq} &= -\omega_s V_{scd} + \frac{i_q T}{C_{sc}} \end{aligned} \quad (8)$$

and, the dynamics of the DC link can be obtained as

$$\dot{V}_{dc} = -\frac{1}{C_{dc}} (i_{qs} u_q + i_{ds} u_d - i_{dc}) \quad (9)$$

where the capacitance of the line compensator and DC-link can be denoted by  $C_{sc}$  and  $C_{dc}$ , respectively. Using (6)-(8), the relation providing  $I_{dq}$  dependent active and reactive power is obtained as

$$P_s = -\frac{MV_s}{L_s} I_{qr}; Q_s = \frac{V_s^2}{\omega_s L_s} - \frac{MV_s}{L_s} I_{dr} \quad (10)$$

From (10), controlling the rotor side current  $I_{dq}$  with dynamic and adaptive feedback control can effectively mitigate the complex oscillations emerging due to SSCI or SSR accompanied by the line compensator. This can be achieved by considering the control loop as a virtual impedance responding proportionally to the RSC current perturbation due to SSR based oscillations (SSRO). The finite time compensation of this perturbation effectively changes the DFIG impedance, preventing the destabilization of the control loop and consequently mitigating the SSRO.

### B. Limitations of Conventional Damping Controllers

In this sub-section, the key limitations of the conventional damping controllers employed for mitigating the SSRO or SSCI-driven oscillations are discussed. Fig. 2 shows the CSDC structure incorporating the bandpass filter, an amplifier and a phase compensator to generate the control signal [13]. The key limitations of such an approach relying on the predefined bandwidth encompass three key aspects as below.

I) The predefined fixed bandwidth of bandpass filter limits the adaptivity of the control for mitigating SSRO with time-varying frequency components [3]. This imposes frequency-dependent constraints on the controller, where the complex components with out-of-band frequencies could strongly influence the accuracy of input signal for GFLC in wind systems.

II) The time-varying components introduce explicitly complex phase lags. This can deteriorate the performance of the fixed phase compensators ( $[(ST_1 + 1)/(ST_2 + 1)]^2$ ) to compensate for the phase-angle due to the presence of complex modes [3], [9].

III) In extreme conditions, apart from the SSR components, the intricate modes entail frequency interdependence induced by SSCI, inciting more complex oscillations. These modes vary with the operating conditions of the network and

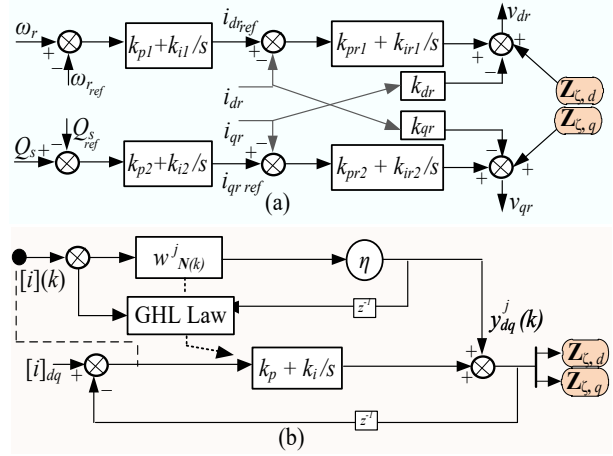


Fig. 3: Proposed method for RSC control of DFIG, (a) RSC control modified with DVIC (b) Structure of proposed method for  $Z_c$ .

contribute to negative damping. Therefore, the control tuned for the specific frequencies of SSR modes may worsen the oscillations mitigation and destabilize the network.

The conventional damping controllers are tuned for a single operating point of the network. The parameters of the control do not update online to accommodate any evolving dynamics of the network. This deteriorates the damping performance for mitigating SSRO, further exacerbating the situation for complex modes amid varying operating conditions. It can therefore be concluded that IBR-dominated networks, specifically integrated with network compensators, imposing the requirement for the control mechanisms to be self-adaptive to accommodate the varying operating conditions of the network.

### III. PROPOSED APPROACH

To address identified issue, we propose a artificial neural networks (ANN) based single-layer feed-forward model-free control mechanism that can mitigate the SSCI in finite time for varying operating conditions of the network. The principle of the proposed approach is similar to that of CSDC and is shown in Fig. 3. The control method is independent on the system states, communication links and prior information of SSCI modes to mitigate the SSRO in finite time. The method uses system state  $x_{Idqr}$  as its input, measures  $\Delta x[k] = x[k] - x[k-1]$ , and adjusts output  $y(k)$  online. The  $y(k)$  is a stabilizing signal injected into the  $dq$  control of the DFIG, strengthening the output impedance of the RSC in finite time. Furthermore, the proposed method works as a dynamic virtual impedance control (DVIC), reshaping the RSC impedance by adjusting the internal gains using generalized Hebbian learning law (GHLL) for any operating condition [11]. The impedance model (IM) of DFIG can be derived from the analytical model discussed in the earlier section as

$$Z_{DFIG} = (Z_m || Z_r) + Z_s \quad (11)$$

where

$$\begin{cases} Z_r(s) = s\hat{L}_m + \frac{s}{s-j\omega_r} (\hat{R}_r + k_{pr} + \frac{k_{ir}}{s-j\omega_0}) \\ Z_m(s) = sM \\ Z_s(s) = \hat{R}_s + s\hat{L}_s \end{cases}$$

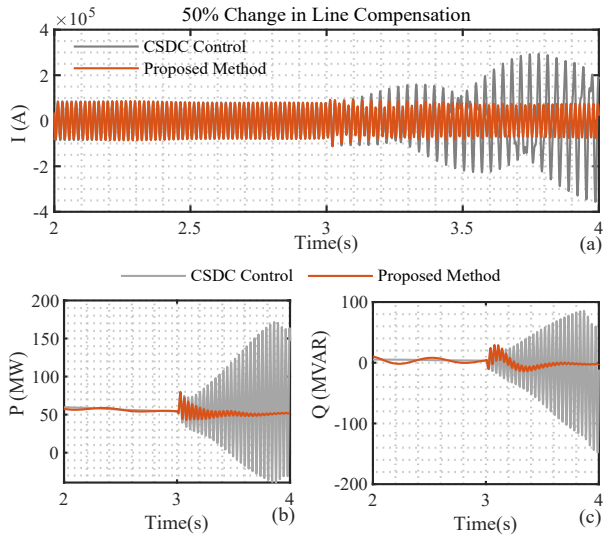


Fig. 4: Comparison of SSRO mitigation with changing line compensation from 20% to 50% at  $t=3$  s, showing (a) the current output of DFIG, (b) active power, (c) reactive power.

Assuming  $\mathbf{Z}_\zeta$  is the output ( $y(k)$ ) of the DVIC as shown in Fig. 3b, the new impedance for the RSC can be updated at each operating state as

$$\mathbf{Z}_{r,(s,z_\kappa)} = s\hat{L}_m + \frac{s}{s - j\omega_r}(\hat{R}_r + k_{pr} + \frac{k_{ir}}{s - j\omega_0} + \mathbf{Z}_\zeta) \quad (12)$$

where  $\hat{L}_m$ ,  $k_{ir}$ ,  $k_{pr}$  are the field excitation inductance, integral, and proportional gains of the RSC loop, respectively.  $z_\kappa$  refers to the operating mode. From (12),  $\mathbf{Z}_\zeta$  can be determined by the mathematical manipulation of GHLL with PI gains as [11]

$$\mathbf{Z}_\zeta = \sum_{\mathbf{N}=1 \dots \eta} [\Delta w_{\mathbf{N}}(k)] \times (k_p I_{dr} + k_i \int I_{qr}) \quad (13)$$

The learning relation between the updated synaptic weights ( $w_{\mathbf{N}}^j(k)$ ) and the corresponding inputs  $x^j[k]$  and output  $y^j[k]$  states can be written as

$$\Delta w_{\mathbf{N}}^j(k) = \eta \left[ y^j(k) \cdot x^j(k) - y^j(k) \sum_{k=1}^n w^j(k) y(k) \right] \quad (14)$$

where  $\eta$  is the learning rate for updated synaptic weights ( $w_{\mathbf{N}}^j(k)$ ) at each interval of “ $j$ ”. From (13) and (14), the final value of the weights is decided when the connection between neurons is strengthened and error is minimized by ensuring an optimum correlation between the reference and output values. Therefore, the training data and learning relation are updated online every time step of the corresponding input state vector and the effect of variations in the input signal is thus mitigated in finite time.

#### IV. TEST SYSTEM AND VIABILITY OF DVIC

This work considers a real network in which SSRO event was triggered by SSCI based oscillations [14]. The parameters of the reported system [14] are adopted here to represent a realistic test case for SSCI-based oscillations. Unlike an SSR-driven event this event is produced by the control interaction

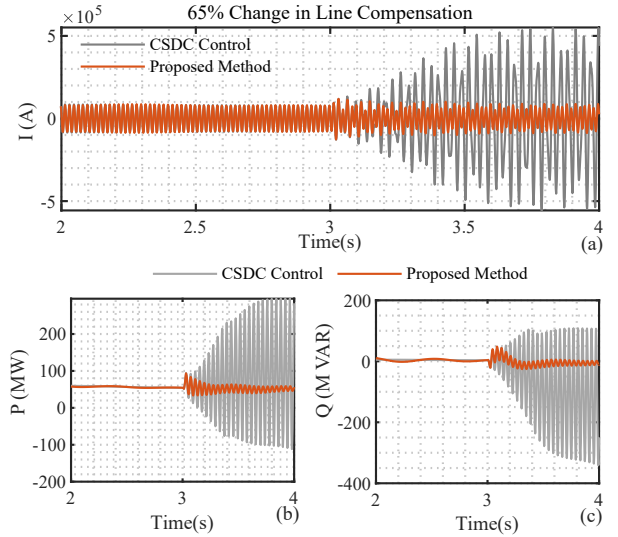


Fig. 5: Comparison of SSRO mitigation with changing line compensation from 20% to 65% at  $t=3$  s, showing (a) the current output of DFIG, (b) active power, (c) reactive power.

of DFIG units. Owing to the control of wind turbine generator (WTG), RSC could behave as a negative resistance with respect to the grid impedance when the system witnesses disturbances, such as variation in the wind speed or change in the network topology. We consider the two aforementioned cases to demonstrate the viability of the proposed DVIC control for real-time grid applications and appraisal the potential for further exploration.

##### A. Test Case 1: Variation in Line Compensation

The performance of the DVIC control is assessed by varying the compensation level of the transmission lines. The control gains, line parameters  $k_p$ ,  $k_i$  and  $w_{\mathbf{N}}$  are taken as 0.012, 0.12 and 0.000015, respectively. The rest of the parameters for WTG and network can be found in [15].

Keeping constant wind speed (9m/s), the line compensation is increased at  $t=3$  s from 20% to 50%. The reference active and reactive power for 20% line compensation is set as 50 MW and 0 MVAR. Initially, both controllers proportionally adjust the active and reactive power to the reference trajectory as shown in Fig. 4. However, upon the activation of line compensation variation at  $t=3$  s, considerable oscillations can be observed in the system response, including active and reactive power. A further variation in the intensity of oscillations can be observed in Fig. 5 when greater line compensation variation (from 20% to 65%) was initiated at  $t=3$  s. This variation in the line compensation triggers the SSCI driven oscillations and as can be observed from Fig. 4 and Fig. 5, the CSDC fails to mitigate SSRO. Conversely, the DVIC control mitigates the disturbance in finite time and keeps the reactive power trajectories to the predefined reference. This can be observed from Fig. 6, where the control inputs ( $v_{dq}$ ) are varied in finite time by DVIC weights ( $w_{\mathbf{N}}^j(k)$ ), thereby mitigating the destabilizing effect stemming from SSCI.

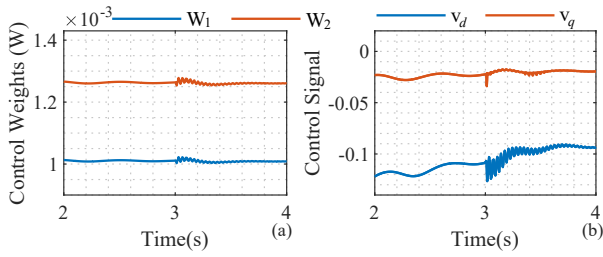


Fig. 6: Time varying control inputs showing (a) DVIC control gain adjustment with oscillation variation (b) control input.

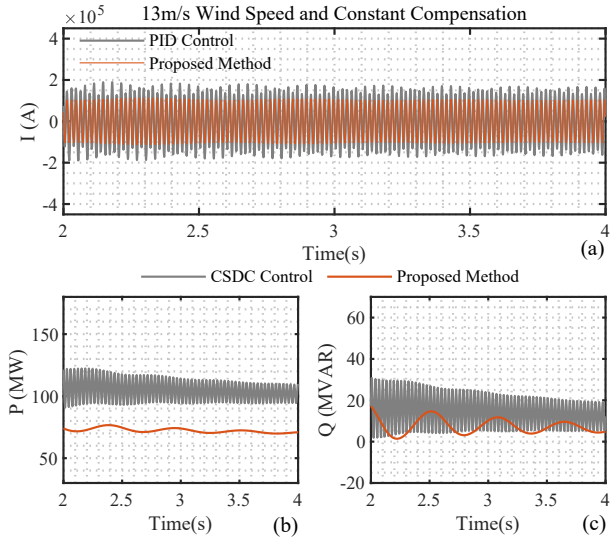


Fig. 7: Comparison of SSRO mitigation in high windspeed of 13m/s showing, (a) the current output of DFIG, (b) The active power, (c) reactive power.

### B. Test Case II: Change in Windspeed

The GSC and RSC control for keeping the variables' trajectories in alignment with the desired reference leads to potential instability under different wind speeds. This triggers the SSCI oscillations, primarily stemming from the asynchronous response of the torque control loop to the inner current loops of the RSC. An illustration of such a case is depicted in Fig. 7, where the performance of both controllers can be analyzed for 13 m/s wind speed. From Fig. 7(b,c), the effect of high wind speed initiating SSCI driven oscillation is minimal using the proposed method. On the other hand, the CSDC shows undesirable oscillations in the current waveform for 13m/s wind speed. The effect can be reflected in the active and reactive power output, showing a significant threat of instability for the system and IBR sources in the network.

## V. CONCLUSIONS

This work proposes a novel RSC control scheme for WTG to enhance the resiliency of  $dq$  axes control loop for mitigating SSCI oscillations. The proposed method works as an auxiliary loop and acts as a dynamic virtual impedance for the DFIG control system. The proposed scheme mitigates the effect of SSCI event in the  $dq$  axes current control loops with improved

steady and, transient system performance. No requirement of prior knowledge of SSCI frequencies, its types and their bandwidth, set apart this work. The proposed method does not deteriorate the nominal operation of the system and responds only when detecting the SSCI event. The simulation results demonstrate the efficacy of the proposed method for different test scenarios and prove its viability for further exploration and real grid applications.

## REFERENCES

- [1] L. Meegahapola *et al.*, "Review on oscillatory stability in power grids with renewable energy sources: Monitoring, analysis, and control using synchrophasor technology," *IEEE Trans. Ind. Electron.*, vol. 68, pp. 519–531, 2021.
- [2] T. Rauhala, A. M. Gole, and P. Järventausta, "Detection of subsynchronous torsional oscillation frequencies using phasor measurement," *IEEE Trans. Power Del.*, vol. 31, no. 1, pp. 11–19, 2016.
- [3] T. Zaman *et al.*, "Multimode synchronous resonance detection in converters dominated power system using synchro-waveforms." in *27th International Conference on Electricity Distribution (CIRED 2023)*, 2023, pp. 3620–3624.
- [4] J. Shair, X. Xie, Y. Li, and V. Terzija, "Hardware-in-the-loop and field validation of a rotor-side subsynchronous damping controller for a series compensated dfig system," *IEEE Trans. Power Del.*, vol. 36, no. 2, pp. 698–709, 2021.
- [5] I. Sami, S. Ullah, N. Ullah, and J.-S. Ro, "Sensorless fractional order composite sliding mode control design for wind generation system," *ISA Transactions*, vol. 111, pp. 275–289, 2021.
- [6] Y. Wang, Q. Wu, R. Yang, G. Tao, and Z. Liu, "H current damping control of dfig based wind farm for sub-synchronous control interaction mitigation," *International Journal of Electrical Power Energy Systems*, vol. 98, pp. 509–519, 2018.
- [7] M. A. Chowdhury and G. M. Shafiqullah, "SSR mitigation of series-compensated dfig wind farms by a nonlinear damping controller using partial feedback linearization," *IEEE Trans. Power Syst.*, vol. 33, no. 3, pp. 2528–2538, 2018.
- [8] M. Ghafouri, U. Karaagac, J. Mahseredjian, and H. Karimi, "SSCI damping controller design for series-compensated dfig-based wind parks considering implementation challenges," *IEEE Trans. Power Syst.*, vol. 34, no. 4, pp. 2644–2653, 2019.
- [9] R. Peña-Alzola, J. Roldán-Pérez, E. Bueno, F. Huerta, D. Campos-Gaona, M. Liserre, and G. Burt, "Robust active damping in lcl-filter-based medium-voltage parallel grid inverters for wind turbines," *IEEE Trans. Power Electron.*, vol. 33, no. 12, pp. 10 846–10 857, 2018.
- [10] X. Wu, S. Feng, P. Jiang, G. Xu, and X. Yang, "An ssr multichannel damping control scheme for tcsc considering multiple operating conditions," *International Trans. Electr. Energy Syst.*, vol. 26, no. 12, pp. 2759–2773, 2016.
- [11] T. Zaman, Z. Feng, S. Mitra, M. Syed, S. Karanki, L. Villa, and G. Burt, "ANN driven fosmc based adaptive droop control for enhanced dc microgrid resilience," *IEEE Trans. Ind. Appl.*, vol. 60, no. 2, pp. 2053–2064, 2024.
- [12] P. Li, L. Xiong, F. Wu, M. Ma, and J. Wang, "Sliding mode controller based on feedback linearization for damping of sub-synchronous control interaction in dfig-based wind power plants," *International Journal of Electrical Power Energy Systems*, vol. 107, pp. 239–250, 2019.
- [13] J. Yao, X. Wang, J. Li, R. Liu, and H. Zhang, "Sub-synchronous resonance damping control for series-compensated dfig-based wind farm with improved particle swarm optimization algorithm," *IEEE Trans. Energy Convers.*, vol. 34, no. 2, pp. 849–859, 2019.
- [14] L. Wang, X. Xie, Q. Jiang, H. Liu, Y. Li, and H. Liu, "Investigation of SSR in practical DFIG-based wind farms connected to a series-compensated power system," *IEEE Trans. Power Syst.*, vol. 30, no. 5, pp. 2772–2779, 2015.
- [15] J. Yao, X. Wang, J. Li, R. Liu, and H. Zhang, "Sub-synchronous resonance damping control for series-compensated dfig-based wind farm with improved particle swarm optimization algorithm," *IEEE Trans. Energy Convers.*, vol. 34, no. 2, pp. 849–859, 2019.